



Impact of low tissue backscattering by optical coherence tomography on endothelial function after drug-eluting stent implantation

Hiroyo Tamaru¹ · Kenichi Fujii¹ · Tsuyoshi Nakata¹ · Masashi Fukunaga¹ · Takahiro Imanaka¹ · Kenji Kawai¹ · Kojiro Miki¹ · Tetsuo Horimatsu¹ · Machiko Nishimura¹ · Ten Saita¹ · Akinori Sumiyoshi¹ · Masahiko Shibuya¹ · Yoshiro Naito¹ · Tohru Masuyama¹ · Masaharu Ishihara¹

Received: 15 May 2018 / Accepted: 27 July 2018 / Published online: 2 August 2018
© Japanese Association of Cardiovascular Intervention and Therapeutics 2018

Abstract

This study evaluated the impact of optical coherence tomography (OCT)-derived low-backscattered tissue on mid-term coronary endothelial function after drug-eluting stent (DES) implantation. Although OCT enables detailed in vivo evaluation of neointimal tissue characterization after DES implantation, its association with physiological vascular healing response is unclear. Thirty-three stable angina pectoris patients underwent OCT examination and endothelial function testing with intracoronary infusion of incremental doses of acetylcholine 8-month after DES implantation in a single lesion of the left anterior descending artery. Neointimal tissue was classified into two patterns based on the predominant OCT light backscatter: high backscatter and low backscatter. Although the presence of uncovered or malapposed stent strut was not associated with the degree of vasoconstriction, the degree of vasoconstriction was significantly greater in the DES with low-backscattered neointima than in the DES without low-backscattered neointima (-32.1 ± 25.7 vs. $-4.1 \pm 20.1\%$, $p=0.003$). Moreover, there was an inverse linear relationship between low backscatter tissue index and degree of vasoconstriction after acetylcholine infusion ($r=0.50$ and $p=0.003$). The endothelium-dependent vasomotor response after 8-month of DES was impaired in patients with low neointimal tissue backscatter on OCT imaging. OCT assessment of low-backscattered tissue may be used as surrogate markers for impairment of endothelial function after DES.

Keywords Drug-eluting stent · Endothelial function · Optical coherence tomography

Introduction

The high spatial resolution of optical coherence tomography (OCT) enables detailed in vivo evaluation of neointimal strut coverage after drug-eluting stent (DES) implantation in the human coronary artery. Previous studies have established the accuracy and reproducibility of OCT in detecting DES strut tissue coverage with thin neointima and strut apposition to the vessel wall after DES deployment [1, 2]. Another capability of OCT is to visualize different tissue morphologies by analyzing the back reflection or backscattering coefficient. Gonzalo et al. [3] have evaluated the morphologic characteristics of stent restenosis by OCT; their classifications of

structure and backscatter on restenotic tissue have been well established. Other studies have reported that OCT imaging identified the low-backscattered neointima in approximately one-third of DES during follow-up period [4, 5]. However, the impact of neointimal tissue characterization by OCT on local vascular healing after DES implantation has not been clarified. Therefore, the aim of this study was to determine the impact of OCT-derived low-backscattered tissue on mid-term coronary endothelial function after DES implantation.

Methods

Patient populations and lesion treatment

Between October 2009 and September 2011, a prospective but non-consecutive series of 33 stable angina pectoris patients underwent OCT examination and endothelial function testing 8 months after percutaneous coronary

✉ Kenichi Fujii
kfujii350@hotmail.com

¹ Division of Cardiovascular Medicine and Coronary Heart Disease, Hyogo College of Medicine, 1-1 Mukogawa-cho, Nishinomiya, Hyogo 6638501, Japan

intervention (PCI) with DES implantation in a de novo single lesion of the left anterior descending artery (LAD). Inclusion criteria were presence of typical stable effort angina or positive stress test and indication for PCI of a single de novo stenosis of $> 75\%$ diameter in a native coronary artery. The exclusion criteria were acute coronary syndrome, $\geq 75\%$ coronary vasoconstriction in response to acetylcholine (Ach) infusion during the pre-intervention test, history of vasospasm, renal insufficiency with creatinine of ≥ 2.0 mg/dL, in-stent restenosis, presence of a lesion at the LAD ostium, diffuse lesions, chronic total occlusions, and left ventricular dysfunction (ejection fraction $< 35\%$). The ethics committee at the Hyogo College of Medicine approved the protocols; written informed consent was obtained from all patients prior to procedure.

After enrollment, the choice of the type of DES [sirolimus-eluting stents (SES), zotarolimus-eluting stent (ZES), everolimus-eluting stent (EES), or biolimus A9-eluting stent (BES)] was at the discretion of the operator and without any specific recommendation. After the initial procedure with one or two DES per patient, oral aspirin (100 mg/day) and clopidogrel (75 mg/day) were given to all patients for at least 12 months. Eight months after stenting, vascular response to DES was evaluated by both OCT and endothelial function testing with Ach infusion.

Evaluation of endothelial function and angiography

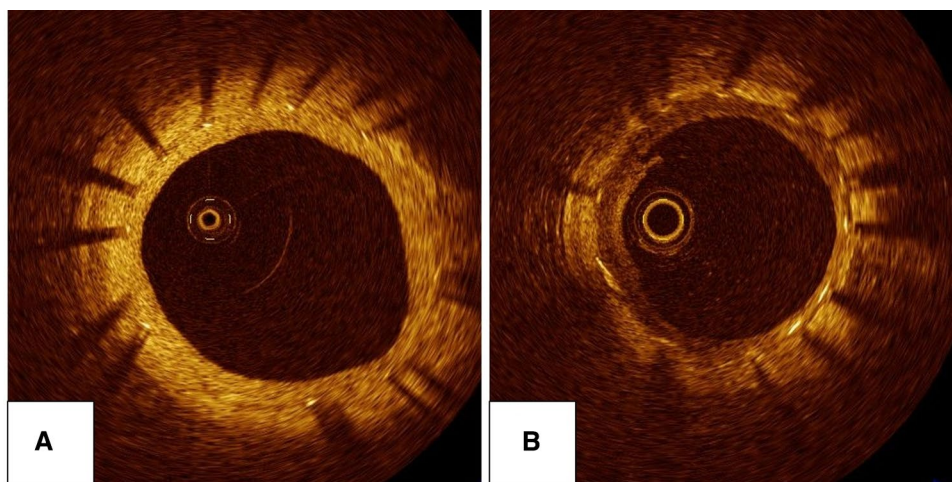
During the initial procedure and at 8 months post-procedure, all anti-anginal agents that influence vasomotor tone, including long-acting nitrates, calcium-channel blockers, statins, and beta-blockers, were withheld for at least 48 h before Ach infusion. After baseline coronary angiography, endothelium-dependent vasomotor response was evaluated by intracoronary infusion of incremental doses of Ach at 10^{-7} and 10^{-6} mol/l (M) for 2 min [6, 7]. At least 3-min intervals were allowed in between Ach infusion. Subsequently, endothelium-independent vasomotor response was tested after an intracoronary bolus infusion of isosorbide dinitrate (ISDN) (3–5 mg). Coronary angiography was repeated after every drug infusion and maximal vasomotor responses to Ach and ISDN infusion were determined by quantitative coronary angiography with a CAAS 5.9.2 system (Pie Medical BV, Maastricht, the Netherlands). Two segments, at 5–10 mm proximal and distal to the stent, were separately chosen for analysis [6, 8]. The same segments were identified by anatomic landmarks and were assessed during each drug infusion measurement. Changes in vessel diameter in response to Ach and ISDN infusion were expressed as percent changes vs. baseline angiograms.

OCT imaging and analysis

On the eighth month of follow-up, OCT examination was performed in all cases as previously described [9]. In brief, a time-domain M2 OCT system (M2 Cardiology Imaging System; LightLab Imaging, Inc., Westford, MA, USA) combined with a 0.016-inch wire-type imaging wire (ImagingWire; LightLab Imaging Inc.) was used in this study. During image acquisition, an over-the-wire occlusion balloon catheter (Helios, LightLab Imaging Inc.) was inflated to 0.4–0.6 atm, and lactated Ringer's solution was infused at 0.5 ml/s from the distal tip of the occlusion balloon catheter to flush out blood from the imaging field. The entire length of the stent was imaged using an automatic pullback device moving at 1 mm/s and the OCT image clearly visualized the stent cross section. Cross-sectional OCT images were analyzed every 1 mm along the segment with stent. Stent and luminal cross-sectional areas (CSA) were measured by manual trace; neointimal hyperplasia (NIH) CSA was calculated as stent CSA minus the luminal CSA. The percentage of NIH CSA was calculated as $\text{NIH CSA} \times 100 / \text{stent CSA}$ [10, 11]. NIH thickness, which was defined as the distance between the center reflection of the strut and the endoluminal surface of the neointima, was measured inside the struts with a line perpendicular to the neointima and strut [12]. An uncovered strut was defined as having an NIH thickness of $0 \mu\text{m}$ [12]. Detachment of the strut from the vessel wall was considered as a malapposed strut (SES $\geq 160 \mu\text{m}$, ZES $\geq 110 \mu\text{m}$, EES $\geq 110 \mu\text{m}$, and BES $\geq 130 \mu\text{m}$) [11, 13]. The percentage of malapposed or uncovered struts was calculated based on the total number of struts in all cross sections of the lesion.

Qualitative tissue characterization of the neointima from the cross-sectional OCT images was also assessed at 1-mm intervals. Neointimal tissue within the stent was classified into two patterns based on the predominant OCT light backscatter: high backscatter (bright) and low backscatter (dark or black) (Fig. 1). Neointimal tissue was classified as low backscatter if neointima is low density, and the line between neointimal layer and intima can be clearly drawn [25]. The longitudinal extent of low-backscattered tissue was assessed as low backscatter tissue index, or the number of serial cross sections with low-backscattered neointima divided by stent length. This quantitative analysis was performed on cross sections with maximum NIH thickness of $\geq 100 \mu\text{m}$, which obtained sufficient amount of neointima for detection of tissue characteristics at the region of maximal %NIH CSA [3, 5, 14, 15]. Additional assessments were based on lumen shape (regular or irregular), presence of intraluminal material in the neointima of the stented lesion, presence of microvessels, presence of extra stent lumen, and dissection in the stented lesion [3,

Fig. 1 Classification of neointimal tissue backscatter on optical coherence tomography. **a** A homogeneous pattern is seen as neointimal tissue with uniform optical properties. **b** Low-backscattered neointimal tissue surrounding stent struts is seen



16, 17]. Intraluminal material was defined as a protruding mass, regardless of size, and extent of signal attenuation. Microvessel was defined as well-delineated low backscattering structures $< 200 \mu\text{m}$ in diameter and with a trajectory within the vessel. Extra stent lumen was defined as a lumen outside the stent on cross section.

Statistical analysis

Statistical analysis was performed with EZR on R commander (Saitama Medical Center, Jichi Medical University, Saitama, Japan). Continuous variables were reported as mean \pm SD. Unpaired Student's *t* tests were used to compare two sets of data with normal distributions. For comparison of continuous variables with more than three sets of data, one-way analysis of variance (ANOVA) was performed. Categorical variables were reported as frequencies and were compared using Chi square test and Fisher's exact test. The relationship between degree of vasoconstriction to Ach and quantitative parameter on OCT was evaluated by Pearson correlation analysis. A *p* value of < 0.05 was considered statistically significant.

Results

Baseline patient, lesion, and procedural characteristics

The baseline characteristics of the patients, lesions, and procedures are shown in Table 1. The average interval between baseline and follow-up studies was 247 ± 82 days. The coronary vasomotor response to incremental doses of Ach and ISDN after 8 months of DES implantation is shown in Fig. 2. In the proximal segment, there was no significant coronary vasoconstriction after intracoronary Ach infusion at 10^{-7} M ($0.84 \pm 10.3\%$, $p = 0.76$) and 10^{-6} M

Table 1 Baseline patient, lesion, and procedural characteristics

Patients (<i>n</i>)	33
Follow-up period (days)	247 ± 82
Age (years)	68 ± 9
Male (<i>n</i>)	25 (76%)
Hypertension (<i>n</i>)	31 (94%)
Dyslipidemia (<i>n</i>)	27 (82%)
Diabetes mellitus (<i>n</i>)	15 (45%)
Current smoking (<i>n</i>)	14 (42%)
Previous coronary angioplasty (<i>n</i>)	10 (30%)
Lesion type	
A/B1	12 (36%)
B2/C	21 (64%)
Stent diameter (mm)	2.9 ± 0.3
Stent length (mm)	20.5 ± 5.1
Stent type (<i>n</i>)	
Sirolimus-eluting stent	8 (24%)
Zotarolimus-eluting stent	9 (27%)
Everolimus-eluting stent	9 (27%)
Biolimus A9-eluting stent	7 (21%)
Concomitant medication (<i>n</i>)	
Aspirin	33 (100%)
Clopidogrel	33 (100%)
Nitrate	8 (24%)
Calcium-channel blocker	15 (45%)
Beta blocker	13 (39%)
ACE-I/ARB	23 (60%)
Statin	21 (64%)

Data are presented as means \pm 1 standard deviation or numbers (%)

ACE-I angiotensin-converting enzyme inhibitor, ARB angiotensin receptor blockers

($-2.35 \pm 10.4\%$, $p = 0.13$). In the distal segment, coronary vasoconstriction was not identified after low-dose Ach infusion ($-3.50 \pm 25.1\%$, $p = 0.33$), but was significant after Ach infusion at 10^{-6} M ($-11.4 \pm 24.2\%$, $p = 0.016$).

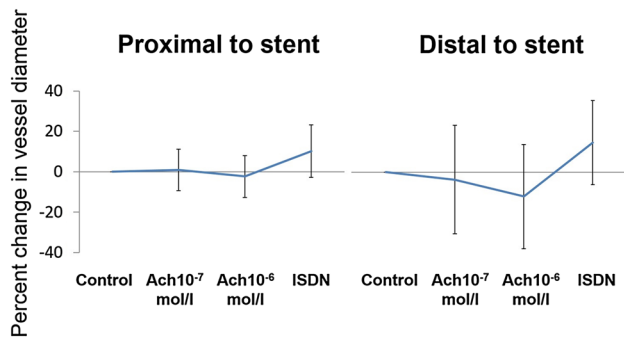


Fig. 2 Coronary vasomotor response to acetylcholine and isosorbide dinitrate. Sites distal to the drug-eluting stent have greater degree of vasoconstriction in the left anterior descending artery. *Ach* acetylcholine, *ISDN* isosorbide dinitrate

Intracoronary ISDN induced a similar grade of vasodilation in both the proximal and distal segments. Vasomotor response to each dose of Ach was not related to the risk factors for cardiovascular disease. However, there was a tendency for greater degree of vasoconstriction after Ach in patients treated with SES and EES than in those treated with ZES and BES (Table 2).

Quantitative and qualitative OCT analysis

Quantitative and qualitative OCT analyses are listed in Table 3. In total, 6593 of 7104 struts (90.7%) were completely covered with neointima. The average neointimal thickness was $155.5 \pm 135.2 \mu\text{m}$, which resulted in approximately 54% of stent struts having neointima of $> 100 \mu\text{m}$. The proportion of uncovered struts and malapposed struts were 7.2 and 1.0%, respectively. In the qualitative OCT analysis, 75.8% of the neointima were classified as high backscatter and 24.2% were classified as low backscatter. In addition, intraluminal material and extra stent lumen were identified in 27.3 and 36.3% of patients, respectively.

Table 2 Coronary vasomotor response to acetylcholine in distal segment in each stent

The degree of vasoconstriction (%)	SES	ZES	EES	BES	<i>p</i> value
Ach 10 ⁻⁷ mol/l	-5.1 ± 2.0	-2.0 ± 12.6	-17.5 ± 27.6	14.5 ± 31.6	0.08
Ach 10 ⁻⁶ mol/l	-19.3 ± 22.1	-4.8 ± 15.4	-22.1 ± 28.0	-3.1 ± 24.8	0.12
ISDN	-12.8 ± 11.4	8.4 ± 10.4	14.4 ± 19.2	20.2 ± 34.0	0.71

Data are presented as means \pm 1 standard deviation

Ach acetylcholine, *BES* biolimus A9-eluting stent, *EES* everolimus-eluting stent, *ISDN* isosorbide dinitrate, *SES* sirolimus-eluting stent, *ZES* zotarolimus-eluting stent

Association between coronary vasomotor response and OCT findings

After 10^{-6} M of Ach infusion in the distal segment, there was no significant correlation between any of the quantitative OCT parameters, including mean lumen CSA, mean stent CSA and percentage of NIH CSA, and the degree of vasoconstriction (Table 4); in addition, the percentage of uncovered or malapposed struts was not associated with the degree of vasoconstriction. Similarly, the degree of vasoconstriction after Ach infusion in the distal segment did not show marked difference, regardless of the presence of abnormal findings on OCT, including irregular lumen shape, intramural material, microvessel, and extra stent lumen appearance. However, after 10^{-6} M of Ach infusion in the distal segment, vasoconstriction was significantly greater in the DES with low-backscattered neointima than in the DES without low-backscattered neointima (-32.1 ± 25.7 vs. $-4.1 \pm 20.1\%$, $p = 0.003$, Fig. 3). Moreover, there was an inverse linear relationship between low backscatter tissue index and degree of vasoconstriction after Ach infusion in the distal segment ($r = 0.50$, $p = 0.003$, Fig. 4).

Discussion

The main findings of this study were as follows. The endothelium-dependent vasomotor response was impaired in DES containing low-backscattered neointima compared with DES without low-backscattered neointima. No significant correlation was identified between any of the quantitative OCT parameters and degree of vasoconstriction after Ach. To the best of our knowledge, this is the first study to demonstrate the correlation between neointimal tissue morphology assessed by OCT and delayed recovery of endothelial function after vascular injury from DES implantation.

OCT has recently been introduced as a higher resolution intravascular imaging method that allows precise assessment of thin neointima after DES implantation, in comparison with other intracoronary imaging modalities. Another advantage of OCT is detection of different neointimal tissue morphologies by analyzing back reflection or

Table 3 Quantitative and qualitative OCT analysis at 8 months after PCI

Mean lumen CSA (mm ²)	6.2 ± 2.3
Mean stent CSA (mm ²)	7.6 ± 2.0
Mean neointimal CSA (mm ²)	1.6 ± 1.4
Mean neointimal thickness (μm)	155 ± 135
Maximum NIH (μm)	513 ± 324
Minimum NIH (μm)	11 ± 25
Percent NIH CSA (%)	20.4 ± 15.1
Strut level analysis	
Number of overall stent struts (n)	7104
Number of uncovered struts (n)	511 (7%)
Number of malapposed struts (n)	69 (1%)
Cross-sectional level analysis	
Number of cross sections (n)	710
Number of CSA with maximum NIH ≥ 100 μm (n)	579 (82%)
Number of cross sections with high backscatter (n)	536 (93%)
Number of cross sections with low backscatter (n)	43 (7%)
Neointimal tissue	
High back scatter	25 (76%)
Low back scatter	8 (24%)
Lumen shape	
Regular	27 (82%)
Irregular	6 (18%)
Intraluminal material	9 (27%)
Microvessels	6 (18%)
Extra stent lumen appearance	12 (36%)
Dissection	0 (0%)

Data are presented as means ± 1 standard deviation or numbers (%)

CSA cross-sectional area, NIH neointimal hyperplasia, OCT optical coherence tomography, PCI percutaneous coronary intervention

Table 4 Relationship between quantitative OCT parameters and vasoconstriction to acetylcholine in the distal segment

	Correlation coefficient (95% CI)	p value
Mean lumen CSA	0.14 (-0.22 to 0.46)	0.46
Mean stent CSA	0.31 (-0.037 to 0.59)	0.08
Mean neointimal CSA	0.21 (-0.14 to 0.52)	0.23
Mean neointimal thickness	0.056 (-0.29 to 0.39)	0.76
Percent NIH CSA	0.16 (-0.20 to 0.47)	0.39
Percent of uncovered struts	0.050 (-0.30 to 0.39)	0.76
Percent of malapposed struts	0.008 (-0.34 to 0.35)	0.96

CI confidence interval, CSA cross-sectional area, NIH neointimal hyperplasia, OCT optical coherence tomography

backscattering coefficient. Gonzalo et al. previously demonstrated various OCT patterns of restenosed tissue after stent implantation [3]. In addition, Yonetsu et al. suggested that low-backscattered neointima was found in 37% of DES that were deployed for less than 9 months [5]. In this study,

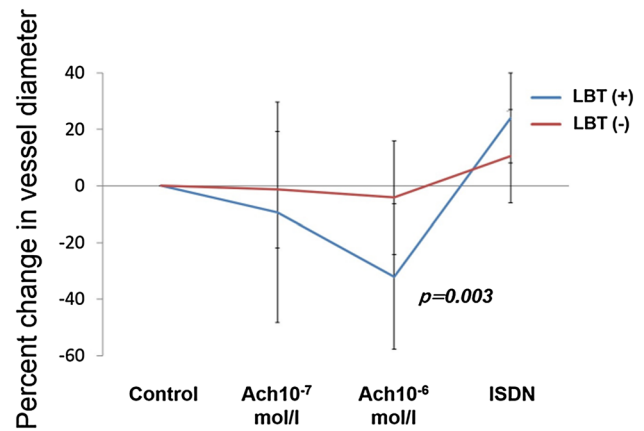


Fig. 3 Coronary vasomotor response to acetylcholine with or without low-backscattered tissue. Distal to the drug-eluting stent, there is a greater degree of vasoconstriction after acetylcholine infusion in the presence of low-backscattered tissue compared to drug-eluting stent without low-backscattered tissue. Ach acetylcholine, ISDN isosorbide dinitrate, LBT low-backscattered tissue

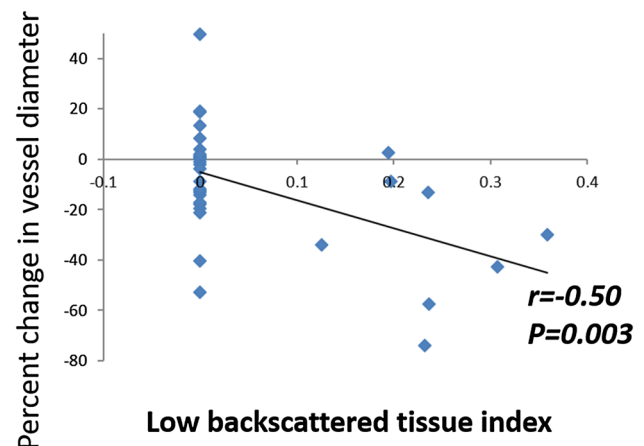


Fig. 4 Relationship between low backscatter tissue index and degree of vasoconstriction after acetylcholine in the distal segment. In the distal stent segment, low backscatter tissue index is inversely correlated with coronary vasomotor response to incremental doses of acetylcholine ($r = -0.50$, $p = 0.003$)

low-backscattered neointima was observed in 24.2% of DES. However, the question remains as to whether the presence of low-backscattered tissue can be used as a surrogate for vessel healing after DES implantation. Previous ex vivo study and review article have reported that these low-backscattered neointima on OCT imaging represented fibrin accumulation, organized thrombus, and excessive inflammation, which are characterized by delayed healing after DES implantation [18, 19, 26, 27]. The current study demonstrated that the vasomotor response to Ach was impaired in DES containing low-backscattered neointima than in DES not containing low-backscattered neointima. The results of the current

study confirmed previous findings that the presence of low-backscattered neointima on OCT imaging may be a marker of impaired vascular healing and may be used as surrogate markers for impairment of vascular endothelial function after DES.

In the present study, there was no association between the degree of vasoconstriction after Ach and the presence of other abnormal findings on OCT, including irregular lumen shape, intramural material, and microvessels. Because OCT provides intravascular images with approximately 10 μm of axial resolution, the presence of stent strut coverage on OCT may be used as a surrogate marker of endothelial coverage after DES implantation. However, although OCT offers higher resolution than any other available imaging modality, it does not have sufficient resolution to visualize re-endothelialization in the form of a 5- μm -thick cellular monolayer [20]. A previous *ex vivo* study also reported that there was a discrepancy in the evaluation of the neointima on the surface of stent strut, especially when neointimal thickness was $< 80 \mu\text{m}$ [21]. Therefore, even if OCT was able to visualize uncovered stent struts, some struts could still be re-endothelialized. In addition, OCT may not be able to distinguish between small amounts of neointima and tissue structures, such as fibrin, on stent struts of the DES. The lack of functional assessment of the endothelium is another potential limitation of OCT in the assessment of stent strut coverage. Endothelial function after DES implantation is generally estimated by measuring coronary vasomotor reactivity in response to Ach infusion [22, 23]. In accordance with the present study, we have recently reported that the degree of coronary vasoconstrictive responses to Ach after stent implantation was different between the first-generation DES and second-generation DES, although the percentage of neointimal strut coverage on OCT was similar [24]. In present study, however, there was a tendency for greater the degree of coronary vasoconstrictive responses to Ach in patients treated with EES than in those treated with ZES and BES. Although the precise reason for this finding is unclear, it is known that Zotarolimus and Biolimus A9 are more lipophilic drugs and would quickly bind to the target, lipid rich, tissue on release. Moreover, abluminal biodegradable polymer in BES could contributed to suppression of endothelial impairment after DES [28, 29]. The results of our present study suggested that neointimal tissue characterization, rather than the presence of neointimal coverage, should be performed during OCT imaging for evaluation of vascular healing after DES implantation. Although the clinical impact of the delayed recovery of endothelial function after DES implantation on the clinical outcomes is still under discussion, most studies to date point toward smaller degree of coronary vasoconstrictive responses to Ach with the new-generation DES, because of the lipophilicity of newer drugs with a better biocompatibility of the polymers.

Also, it seems that newer generation DESs such as BES, with a demonstrated better preservation of endothelial function, may cause neoatherosclerosis to a lesser degree, authorizing a greater reduction of stent thrombosis rates. These data may support the potential clinical benefit of the better recovery of endothelial function after DES implantation.

Study limitations

This study had several limitations. First, this was a retrospective data analysis with relatively small number of patient population. Nevertheless, we evaluated over 7000 stent struts by OCT and vasomotor response was estimated by infusing two different doses of Ach. Second, OCT examinations were not performed immediately after stent implantation. Therefore, it is unclear whether the incomplete apposition identified by OCT was persistent or was acquired late. Third, stents with mean neointimal thickness of $< 100 \mu\text{m}$ were excluded because of the difficulty in analyzing the neointimal characteristics. Forth, data regarding coronary vasomotor response to Ach immediately after DES implantation because to precisely identify the same segment before stent implantation were demanding.

Conclusions

The endothelium-dependent vasomotor response after 8 months of DES implantation was impaired in patients with low neointimal tissue backscatter on OCT. OCT assessment of low-backscattered tissue may be used as surrogate markers for impairment of endothelial function after DES.

Acknowledgements The authors thank the staff in the catheterization laboratory in Hyogo College of Medicine for their excellent assistance during the study.

Compliance with ethical standards

Conflict of interest The authors report no financial relationships or conflicts of interest regarding the content herein.

References

1. Iwasaki M, Otake H, Shinke T, Nakagawa M, Hariki H, Osue T, et al. Vascular responses in patients with and without diabetes mellitus after everolimus-eluting stent implantation. *Circ J*. 2014;78:2188–96.
2. Matsumoto D, Shite J, Shinke T, Otake H, Tanino Y, Ogawara D, et al. Neointimal coverage of sirolimus-eluting stents at 6-month follow-up: evaluated by optical coherence tomography. *Eur Heart J*. 2007;28:961–7.
3. Gonzalo N, Serruys PW, Okamura T, van Beusekom HM, Garcia-Garcia HM, van Soest G, et al. Optical coherence tomography patterns of stent restenosis. *Am Heart J*. 2009;158:284–93.

4. Tada T, Kadota K, Hosogi S, Miyake K, Amano H, Nakamura M, et al. Association between tissue characteristics evaluated with optical coherence tomography and mid-term results after paclitaxel-coated balloon dilatation for in-stent restenosis lesions: a comparison with plain old balloon angioplasty. *Eur Heart J Cardiovasc Imaging*. 2014;15:307–15.
5. Yonetsu T, Kim JS, Kato K, Kim SJ, Xing L, Yeh RW, et al. Comparison of incidence and time course of neoatherosclerosis between bare metal stents and drug-eluting stents using optical coherence tomography. *Am J Cardiol*. 2012;110:933–9.
6. Minami Y, Kaneda H, Inoue M, Ikutomi M, Morita T, Nakajima T. Endothelial dysfunction following drug-eluting stent implantation: a systematic review of the literature. *Int J Cardiol*. 2013;165:222–8.
7. Mitsutake Y, Ueno T, Yokoyama S, Sasaki K, Sugi Y, Toyama Y, et al. Coronary endothelial dysfunction distal to stent of first-generation drug-eluting stents. *JACC Cardiovasc Interv*. 2012;5:966–73.
8. Fujii K, Kawasaki D, Oka K, Akahori H, Fukunaga M, Sawada H, et al. Endothelium-dependent coronary vasomotor response and neointimal coverage of zotarolimus-eluting stents 3 months after implantation. *Heart*. 2011;97:977–82.
9. Fujii K, Masutani M, Okumura T, Kawasaki D, Akagami T, Ezumi A, et al. Frequency and predictor of coronary thin-cap fibroatheroma in patients with acute myocardial infarction and stable angina pectoris a 3-vessel optical coherence tomography study. *J Am Coll Cardiol*. 2008;52:787–8.
10. Kim BK, Kim JS, Park J, Ko YG, Choi D, Jang Y, et al. Comparison of optical coherence tomographic assessment between first- and second-generation drug-eluting stents. *Yonsei Med J*. 2012;53:524–9.
11. Won H, Kim JS, Shin DH, Kim BK, Ko YG, Choi D, et al. Relationship between endothelial vasomotor function and strut coverage after implantation of drug-eluting stent assessed by optical coherence tomography. *Int J Cardiovasc Imaging*. 2014;30:263–70.
12. Takano M, Inami S, Jang IK, Yamamoto M, Murakami D, Seimiya K, et al. Evaluation by optical coherence tomography of neointimal coverage of sirolimus-eluting stent three months after implantation. *Am J Cardiol*. 2007;99:1033–8.
13. Kim BK, Kim JS, Oh C, Ko YG, Choi D, Jang Y, et al. Major determinants for the uncovered stent struts on optical coherence tomography after drug-eluting stent implantation. *Int J Cardiovasc Imaging*. 2012;28:705–14.
14. Vergallo R, Yonetsu T, Uemura S, Park SJ, Lee S, Kato K, et al. Correlation between degree of neointimal hyperplasia and incidence and characteristics of neoatherosclerosis as assessed by optical coherence tomography. *Am J Cardiol*. 2013;112:1315–21.
15. Yonetsu T, Kato K, Kim SJ, Xing L, Jia H, McNulty I, et al. Predictors for neoatherosclerosis: a retrospective observational study from the optical coherence tomography registry. *Circ Cardiovasc Imaging*. 2012;5:660–6.
16. Konishi A, Shinke T, Otake H, Takaya T, Nakagawa M, Inoue T, et al. Favorable vessel healing after nobori biolimus A9-eluting stent implantation-6- and 12-month follow-up by optical coherence tomography. *Circ J*. 2014;78:1882–90.
17. Lee SY, Shin DH, Mintz GS, Kim JS, Kim BK, Ko YG, et al. Optical coherence tomography-based evaluation of in-stent neoatherosclerosis in lesions with more than 50% neointimal cross-sectional area stenosis. *EuroIntervention*. 2013;9:945–51.
18. Nagai H, Ishibashi-Ueda H, Fujii K. Histology of highly echolucent regions in optical coherence tomography images from two patients with sirolimus-eluting stent restenosis. *Catheter Cardiovasc Interv*. 2010;75:961–3.
19. Nakano M, Vorpahl M, Otsuka F, Taniwaki M, Yazdani SK, Finn AV, et al. Ex vivo assessment of vascular response to coronary stents by optical frequency domain imaging. *JACC Cardiovasc Imaging*. 2012;5:71–82.
20. Fujii K, Hao H, Masuyama T. Can optical coherence tomography findings be used as surrogates for vessel healing after drug-eluting stent implantation? *Circ J*. 2014;78:1826–7.
21. Murata A, Wallace-Bradley D, Tellez A, Alviar C, Aboodi M, Sheehy A, et al. Accuracy of optical coherence tomography in the evaluation of neointimal coverage after stent implantation. *JACC Cardiovasc Imaging*. 2010;3:76–84.
22. Hofma SH, van der Giessen WJ, van Dalen BM, Lemos PA, McFadden EP, Sianos G, et al. Indication of long-term endothelial dysfunction after sirolimus-eluting stent implantation. *Eur Heart J*. 2006;27:166–70.
23. Kim JW, Suh SY, Choi CU, Na JO, Kim EJ, Rha SW, et al. Six-month comparison of coronary endothelial dysfunction associated with sirolimus-eluting stent versus Paclitaxel-eluting stent. *JACC Cardiovasc Interv*. 2008;1:65–71.
24. Nakata T, Fujii K, Fukunaga M, Shibuya M, Kawai K, Kawasaki D, et al. Morphological, functional, and biological vascular healing response 6 months after drug-eluting stent implantation: a randomized comparison of three drug-eluting stents. *Catheter Cardiovasc Interv*. 2016;88:350–7.
25. Tanaka N, Terashima M, Rathore S, et al. Different patterns of vascular response between patients with or without diabetes mellitus after drug-eluting stent implantation: optical coherence tomographic analysis. *JACC Cardiovasc Interv*. 2010;3:1074–9.
26. Nakazawa G, Shinke T, Ijichi T, et al. Comparison of vascular response between durable and biodegradable polymer-based drug-eluting stents in a porcine coronary artery model. *EuroIntervention*. 2014;10:717–23.
27. Hoymans VY, van Dyck CJ, Haine SE, et al. Long-term vascular responses to Resolute[®] and Xience V[®] polymer-based drug-eluting stents in a rabbit model of atherosclerosis. *J Interv Cardiol*. 2014;27:381–90.
28. Hamilos M, Sarma J, Ostojic M, et al. Interference of drug-eluting stents with endothelium-dependent coronary vasomotion: evidence for device-specific responses. *Circ Cardiovasc Interv*. 2008;1:193–200.
29. Sumida A, Gogas BD, Nagai H, et al. A comparison of drug eluting stent biocompatibility between third generation NOBORI biolimus A9-eluting stent and second generation XIENCE V everolimus-eluting stent in a porcine coronary artery model. *Cardiovasc Revasc Med*. 2015;16:351–7.